



Evidence for a physical linkage between galactic cosmic rays and regional climate time series

Charles A. Perry

US Geological Survey, 4821 Quail Crest Place, Lawrence, KS 66049, USA

Received 17 November 2006; received in revised form 22 February 2007; accepted 23 February 2007

Abstract

The effects of solar variability on regional climate time series were examined using a sequence of physical connections between total solar irradiance (TSI) modulated by galactic cosmic rays (GCRs), and ocean and atmospheric patterns that affect precipitation and streamflow. The solar energy reaching the Earth's surface and its oceans is thought to be controlled through an interaction between TSI and GCRs, which are theorized to ionize the atmosphere and increase cloud formation and its resultant albedo. High (low) GCR flux may promote cloudiness (clear skies) and higher (lower) albedo at the same time that TSI is lowest (highest) in the solar cycle which in turn creates cooler (warmer) ocean temperature anomalies. These anomalies have been shown to affect atmospheric flow patterns and ultimately affect precipitation over the Midwestern United States. This investigation identified a relation among TSI and geomagnetic index aa (GI-AA), and streamflow in the Mississippi River Basin for the period 1878–2004. The GI-AA was used as a proxy for GCRs. The lag time between the solar signal and streamflow in the Mississippi River at St. Louis, Missouri is approximately 34 years. The current drought (1999–2007) in the Mississippi River Basin appears to be caused by a period of lower solar activity that occurred between 1963 and 1977. There appears to be a solar “fingerprint” that can be detected in climatic time series in other regions of the world, with each series having a unique lag time between the solar signal and the hydroclimatic response. A progression of increasing lag times can be spatially linked to the ocean conveyor belt, which may transport the solar signal over a time span of several decades. The lag times for any one region vary slightly and may be linked to the fluctuations in the velocity of the ocean conveyor belt.

Published by Elsevier Ltd. on behalf of COSPAR.

Keywords: Galactic cosmic rays; Regional climate time series; Sun–Earth climate; Mississippi River Basin streamflow

1. Introduction

Climate prediction is still in its infancy compared with weather prediction which has made substantial advances in the last decade (Mass and Kuo, 1998). Weather occurs on a time scale of hours to days, which allows for quick and continuous verification of forecast models and subsequent improvement. Climate prediction moves at a slower pace and occurs over a broad spectrum of time and space making predictions more difficult to verify and more difficult to improve. Verification comes either at an expense of months to years or historic data must be used to hindcast. Hindcasting often involves the use of statistical rela-

tions that may or may not relate to physical processes. Weather prediction skills have improved with improving data collection, better understanding of all physical processes involved, and improved computing power. As during the development of weather prediction, climate prediction currently (2007) is most accurate in the shortest terms, weeks to months, and to a certain extent, to seasons. Beyond the annual cycle of the seasons, climate prediction currently is at a level similar to weather forecasting decades ago, which may be no better than simple persistence.

Important advancements have been made, for example, in understanding the processes of the El Niño/La Niña phenomena and the effects of this tropical variation on regional climates (Latif et al., 1994). Other relations between ocean temperatures and persistent atmospheric features have been developed and are improving seasonal

E-mail address: cperry@usgs.gov

forecasts of climate (McCabe and Dettinger, 1999). Work also has been done on multidecadal drought frequency in the United States using the Pacific Decadal Oscillation (PDO) and the Atlantic Multidecadal Oscillation (AMO) (McCabe et al., 2004). However, long-term (multiyear) predictions of climate are suffering from the same shortcomings that weather predictions once endured, insufficient data, unknown physical processes, and insufficient models. This paper will discuss the physical processes that may be the linkage between solar variability and climate, which could be used to improve predictions.

Speculation of continental drift preceded its proof by more than half a century. The basic processes were known or speculated for considerable time before a key discovery (magnetic structure of sea-floor spreading) finally provided proof (Vine and Matthews, 1963) of a mechanism that led to a better understanding of a complex process. A similar situation may exist for climate prediction. This paper focuses on physical processes that are still considered controversial but may be playing a larger roll than previously suspected.

Some of these physical processes have an extraterrestrial origin (solar) but have been shown to have a statistically significant effect on a regional climatic scale (Perry, 2006). The solar effect on climate has been the most problematic issue for centuries. For example, significant correlations between sunspots and elevations of Lake Victoria in Africa (Brooks, 1923) went out of phase and vanished entirely when longer time series became available. This failure may well be a function of the chosen lag time between the solar forcing function and climatic response which is usually not greater than a few years. Nearly, all solar/climate correlations have suffered from lack of physical connections and have proven to be inaccurate when put to the test of prediction. Arguments against solar forcing of cli-

mate are: (1) insufficient changes in solar brightness; (2) correlation breakdowns and sign changes; (3) timing problems between cause (solar changes) and effect (climate variations); and (4) the lack of solar/terrestrial theories to account for any postulated long-term changes (Hoyt and Shatten, 1997).

This paper examines the combined effect of the modulation of galactic cosmic rays (GCRs), and their potential effect on cloud formation, changes in total solar irradiance (TSI) flux, changes in oceanic temperatures, the ocean conveyor belt system, and the effect of ocean temperatures on persistent atmospheric patterns that dictate regional climatic time series. In this paper, geomagnetic index aa (GI-AA) is used as a proxy for GCR flux. The combination of these factors into a viable climatic predictor is demonstrated by examining a streamflow time series of a sensitive region (to atmospheric patterns) of North America, the Mississippi River Basin, as well as climatic time series of other regions in the world.

The Mississippi River Basin upstream from St. Louis, Missouri, includes both the upper Mississippi River and the Missouri River drainages (Fig. 1). This area also includes a large part of the Nation's grain-producing acreage. The Rocky Mountains form an effective moisture barrier to the west. The major source of moisture is the Gulf of Mexico which lies to the south and east. Large amounts of precipitation occur in the Mississippi River Basin only when near-surface wind patterns bring moisture-laden air from the Gulf of Mexico. For this to occur, upper-level winds must be from the southwest over the central part of North America. Dry conditions result in the basin when upper-level winds are from the northwest. This single-moisture-source feature of the Mississippi River Basin makes it a good area to test a solar/climate connection.

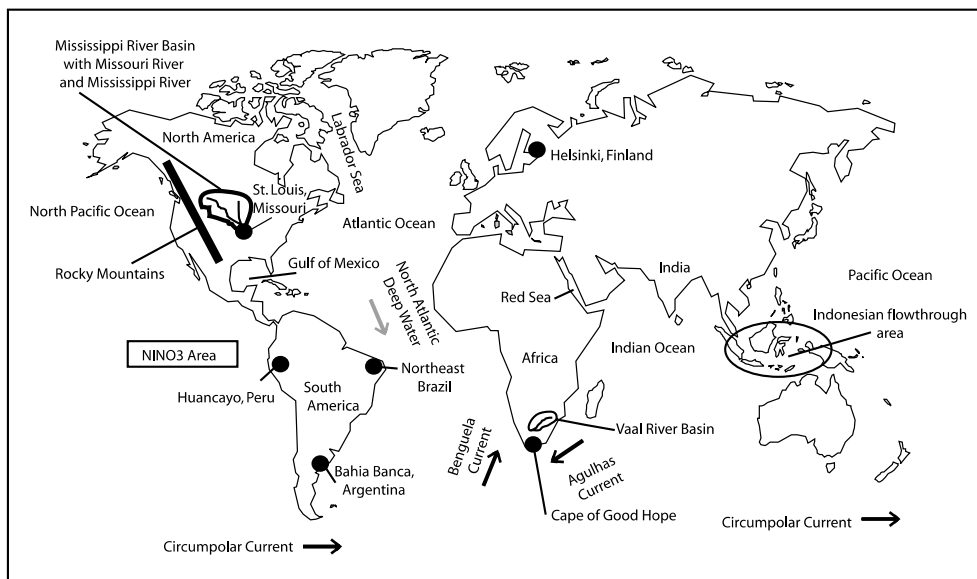


Fig. 1. General location map. (While major ocean currents have been simplified here, they are updated in Fig. 11.)

2. Solar/climate connections

Several mechanisms recently have been postulated for solar activity/climate responses. Roldugin and Tinsley (2004) show atmospheric transmission variations of several percent in nominally clear air are found to accompany solar wind events that affect the flow of vertical current density in the global electric circuit. Also, changes in ultraviolet radiation on the order of 10–20% over the solar cycle show a connection with 11-year oscillations in geopotential height variations through absorption of energy by stratospheric ozone (Shindell et al., 1999). Recent experiments by Svensmark et al. (2007) demonstrate that the production of new aerosol particles is proportional to the negative ion density under experimental conditions similar to those found in the lower troposphere over oceans. This study shows that cosmic rays have a catalytic effect on the nucleation of cloud droplets. GCR flux variations and their potential to affect the amount of albedo from cloud cover may have an important influence on the amount of energy that reaching the Earth's surface and lower troposphere.

3. Galactic cosmic rays and clouds

Galactic cosmic rays (GCRs) are known to be the principal agents of ionization in the atmosphere above 1 km (Palle et al., 2004). This has led to the suggestion that cloud formation may be affected by GCRs through an enhanced production of charged aerosols that may grow to become cloud condensation nuclei. Because the cosmic ray flux on Earth is strongly modulated by solar activity, in the sense that increased solar activity leads to a reduction in cosmic ray flux, if cosmic rays do affect cloudiness, they could provide a link through which solar activity affects climate (Palle et al., 2004).

An earlier study by Svensmark and Friis-Christensen (1997) suggested that total cloud cover over the mid-latitude oceans was correlated with cosmic ray flux during the period 1984–91. However, a study by Kernthaler et al. (1999) led to criticism of their methods and conclusions when correlations weakened after 1991. In a later study of low clouds and GCRs, Palle et al. (2004) noted a correlation of $R = 0.75$ between detrended global low-cloud data and GCRs during the period 1983–2001. The degree of correlation between GCRs and low clouds varied according to latitude, with Palle and Butler (2000) finding stronger correlations in the mid-latitude and equatorial belts and weaker correlations in the polar regions. The results of these and other studies (Sun and Bradley, 2002) show mixed results and point out some problems with actually quantifying low- and mid- to high-level clouds. However, strong evidence that GCRs do have an effect on cloudiness remains, and therefore, the albedo of certain areas of the globe could be modified by GCRs resulting in changes in the amounts of solar energy being absorbed by the oceans.

4. Modulation of galactic cosmic rays

The relations among the GCR flux, magnetic properties of the earth, and solar cycles are well established (Van Allen, 1993). Prior to 1936, however, GCR flux data were not available, therefore it was necessary to use other solar-activity-related parameters as GCR proxies, such as sunspot number or the GI-AA as defined by Mayaud (1972). The GI-AA has been determined from magnetograph readings in the northern and southern hemispheres since 1868. This record has been extended back to 1844 using magnetic measurements in Helsinki, Finland (Nevanlinna, 2004). Others have used the GI-AA as a proxy for GCR flux in climate studies (Stuiver and Quay, 1980; Cliver et al., 1998). In the graphs and correlations to follow, reconstructed geomagnetic data 1844–1867 was used in the graphical comparisons while observed data back to 1868 was used for statistical correlations.

As the solar cycle intensifies (stronger solar wind, stronger interplanetary magnetic field (IMF), higher sunspot number, and higher irradiance), variations of the Earth's magnetic field as represented by the GI-AA also increase. At times of higher solar activity, less GCRs are able to enter the solar system. Not only does the stronger solar wind reduce GCR flux near Earth, it tends to increase the value of the GI-AA. Using data from National Geophysical Data Center (2006a,b,c), there is a good inverse relation between the GI-AA and GCRs measured at Huancayo, Peru, where $R = -0.75$ (Fig. 2) and between sunspots and GCRs where $R = -0.79$ (Fig. 3) The net result is that as solar activity increases, GCR ionization of the Earth's atmosphere decreases. Assuming that the connection between GCRs and low clouds is viable, increased solar activity could result in fewer low-level clouds and a larger amount of solar-irradiance energy reaching the Earth's surface.

The interaction of the IMF with the geomagnetic field is complex. Because the Sun's magnetic field exhibits an approximate 22-year cycle (Hale, 1924), the connection or opposition of the magnetic lines of these two bodies results in a different rate of GCR flux during one approxi-

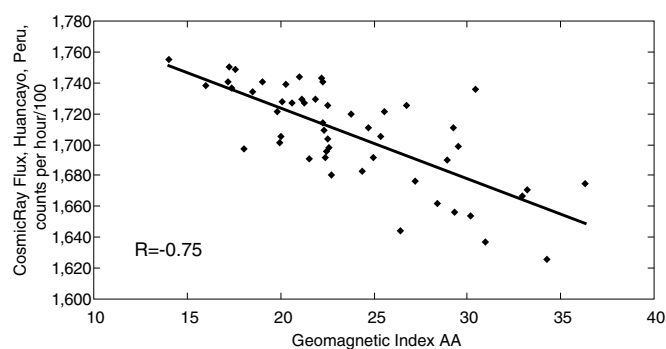


Fig. 2. Observed annual averages of geomagnetic index aa and galactic cosmic ray flux at Huancayo, Peru, 1953–2003. Data are from National Geophysical Data Center (2006a,b).

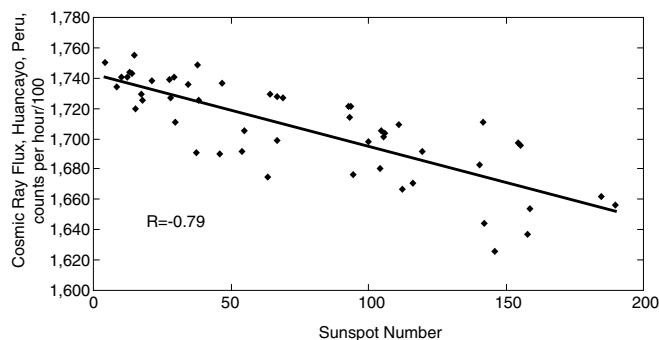


Fig. 3. Observed annual averages of sunspot number and galactic cosmic ray flux at Huancayo, Peru, 1953–2003. Data are from National Geophysical Data Center (2006a,c).

mate 11-year solar-activity cycle and the next. In addition, the time of year can be important as the Earth crosses the plane of the Sun's magnetic equator. Here, the oppositely directed open field lines run parallel to each other and are separated by a thin current sheet known as the "interplanetary current sheet" or "heliospheric current sheet". This sheet is not a perfect plane, but instead undulations spiral out from the Sun and past the Earth, changing the IMF polarity multiple times during the year (Rosenberg and Coleman, 1969). However, generally every other solar cycle has relatively more GCRs reaching the Earth's atmosphere as the radial intensity of GCRs varies on an approximate 22-year cycle (Alania et al., 2005).

The relations among solar variables are not simple or direct. The IMF follows a 22-year variation, whereas irradiance is on an 11-year cycle. The sunspot cycle is not in perfect agreement with total solar irradiance nor is it in perfect agreement with the GCR flux. In Fig. 4, TSI is correlated with the GI-AA, which is used as a proxy for GCR flux in this paper. Solar processes are very complex and are not fully understood as are the processes of GCR enhancement of terrestrial clouds. For this paper, the assumption is made that GI-AA varies inversely with GCR flux and consequentially low-level cloudiness. This assumption allows the use of the approximate 160-year time series of geomag-

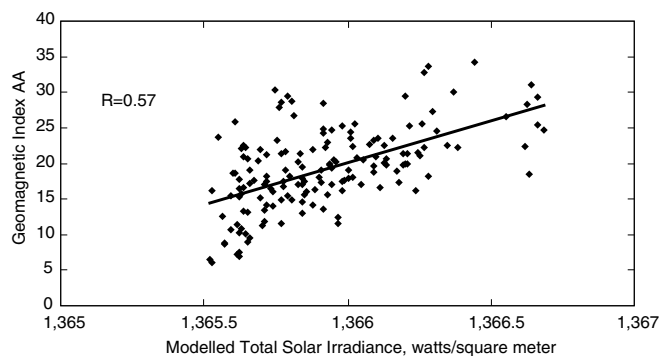


Fig. 4. Modeled annual averages of total solar irradiance and geomagnetic index aa 1844–2000. Total solar irradiance from Lean (2000) and geomagnetic data are from National Geophysical Data Center (2006b).

netic and solar-activity variations to provide information on GCR flux.

5. Total solar irradiance

Total solar irradiance (TSI) has been measured in space by several spacecraft since 1978 (Willson, 1997). TSI and the solar activity-cycle are closely related, but like the GCR flux and GI-AA, the connection is not in perfect step with the solar cycle. Sunspot blocking and ephemeral active regions (areas of more intensive spectral irradiance) cause the TSI flux to vary from the sunspot number cycle. However, data on sunspot properties extend back to the early 18th century and can be used to estimate TSI back to the Maunder Minimum (Lean et al., 1995; Lean, 2000; Wang et al., 2005). This modeled TSI data set can be used with the geomagnetic measurements as a proxy for GCR flux during the same time for comparison with climatic time series.

TSI variations (0.1% over an 11-year period) have been thought to be too small to have an effect on global atmospheric temperatures (Foukal, 2003) and that most of the rise in global temperatures is caused by anthropogenic causes. However, the 0.1% variation translates into over 1 watt per square meter at the Earth's surface. Although small, this variation may be large enough to create sea-surface temperature anomalies, especially near the equator where the incident radiation is perpendicular to the surface. In fact, significant correlations exist between TSI and average ocean-temperature data (White et al., 1998).

6. TSI and GCR interaction

Examination of the relation between annual TSI and annual GI-AA used as a proxy for GCRs during the last 160 years (Fig. 4) shows some correlation ($R = 0.57$). More importantly, the interaction between the two processes may give insight to the total amount of energy reaching the Earth's surface at strategic locations. If GCRs can modulate the amount of low clouds and, therefore, the relative albedo at locations where incoming solar irradiance can best be absorbed by the Earth's oceans, this could be a method of amplifying the small TSI signal into a climate-affecting process. As GCR flux increases (decreases), less (more) energy may be allowed to reach the Earth's surface because of an increase (decrease) in albedo. This decrease (increase) in the energy reaching the surface could create cooler (warmer) ocean temperature anomalies, which could affect climate.

7. Ocean temperatures and regional climatic time series

A mechanism for converting a small TSI signal into a regional climate effect was presented by Perry (2006) for which streamflow data from the Mississippi River at St. Louis (US Geological Survey, 1956, 2006) were used as a measure of the climate of the upper Midwestern United

States (Fig. 1). This basin is unique in that it receives most of its moisture from the Gulf of Mexico but only when atmospheric wind patterns are favorable. The effects of more or less solar energy is tracked through a six-step physically linked process where streamflow is a product of regional rainfall, which is physically linked to regional low-level atmospheric vorticity, which in turn is well correlated with jetstream-level vorticity over the North Pacific Ocean. The jetstream vorticity is linked physically with sea-surface temperatures (SSTs) beneath the same region of the ocean, which compare well with tropical Pacific Ocean temperatures lagged 3 years, which although amplitudes are not consistent, the phasing between the TSI and SSTs is consistent. The data used in Perry (2006) covered the approximate period from 1950 through 2000. Even though the individual correlations between intermediate mechanisms varied, the correlation between modeled TSI lagged 3 years and streamflow for the period 1950–2000 was $R = 0.60$ (Fig. 5). Correlations were computed from the mid-year value (June) of the 36-month moving averages for both solar irradiance and streamflow.

However, when the relation is examined prior to 1950, (the streamflow data for the Mississippi River at St. Louis, Missouri, extends back to 1862) the fairly high correlation between TSI and streamflow from 1950 to 2000 becomes much lower. When GI-AA is compared with the Mississippi River flow between 1950 and 2000 and from 1863 to 2000 the same disparity occurs. Correlations of other lag times between TSI and GI-AA were tested, and an interesting feature was noted. In Fig. 6 the R -squared values between TSI and GI-AA and Mississippi River flow showed some power at 10, 22, and 44 years, but by far the strongest correlations were at a lag time of 34 years for GI-AA and 35 years for TSI (Fig. 6). A graphical comparison of GI-AA with Mississippi River flow (36-month moving averages) demonstrates this relation (Fig. 7). This lag time was unexpected, and its validity questioned. However, others have noted a similar length of lagged correlations within the ocean system. Latif (2001) developed a model that predicted the winter North Atlantic Oscillation (NAO) using the tropical Pacific SST anomalies averaged

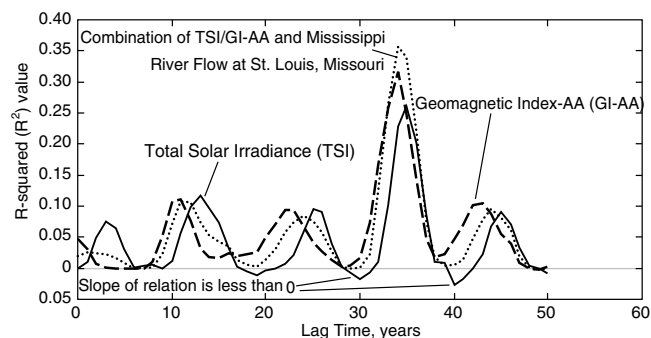


Fig. 6. R -square values for different lag times between June 36-month moving averages of total solar irradiance (TSI), geomagnetic index aa (GI-AA), and combination TSI and GI-AA, and June 36-month moving averages of Mississippi River flow using solar data from the period 1868 to 2000 and flow data from the period 1863 to 2003.

over the NINO3 area (Fig. 1) lagged 35 years. He attributed this lag time to be a feature of an atmospheric bridge between the Pacific and Atlantic Oceans. Ray and Wilson (2003) found lag times of 10, 35, and 13.5 years in salt anomalies leaving the Red Sea and Southern Oscillation Index anomalies.

The relation between GI-AA and 1902–2003 Mississippi River flow (Fig. 7) has a correlation coefficient of $R = 0.56$. The visual correlation between GI-AA and Mississippi River flow shows some interesting features. The amplitudes and the apparent trend in the streamflow data are mirrored in the amplitudes and trend of the GI-AA. The great drought of the 1930s spanned nearly 17 years between the high-flow years of 1927 and 1944. The time between the peaks in the GI-AA was also 17 years, between 1892 and 1909. The wet decade of the 1940s spanned the years 1944–1952 and corresponded to an 8-year period of relatively high GI-AA with peaks 8 years apart, from 1909 to 1917. More recently, streamflow peaks in 1986 and 1994, 8 years apart, corresponded to GI-AA peaks in 1952 and 1960. Currently, 2007, the Mississippi River Basin is in an extended period of drought (1999–2007), which can be traced to a time of low solar activity that occurred during a 14-year period between peaks in GI-AA that occurred from 1963 to 1977.

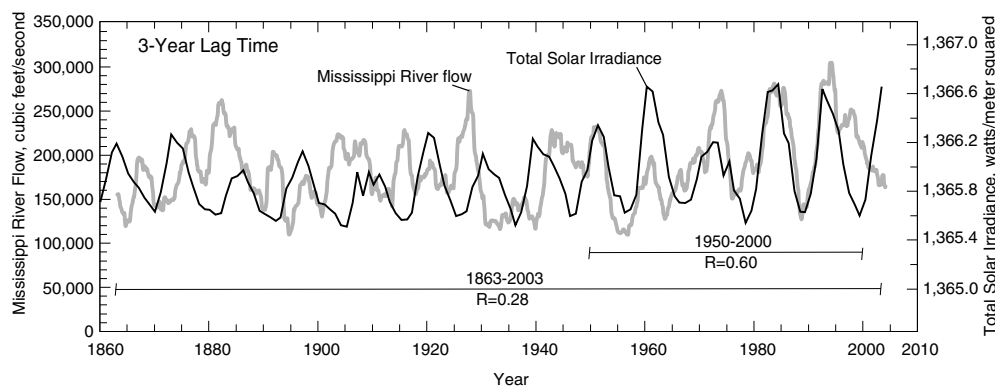


Fig. 5. Thirty-six month moving averages of 1863–2003 Mississippi River flow at St. Louis, Missouri and total solar irradiance (TSI), 3-year lag time. Correlations based on June value of 36-month moving averages.

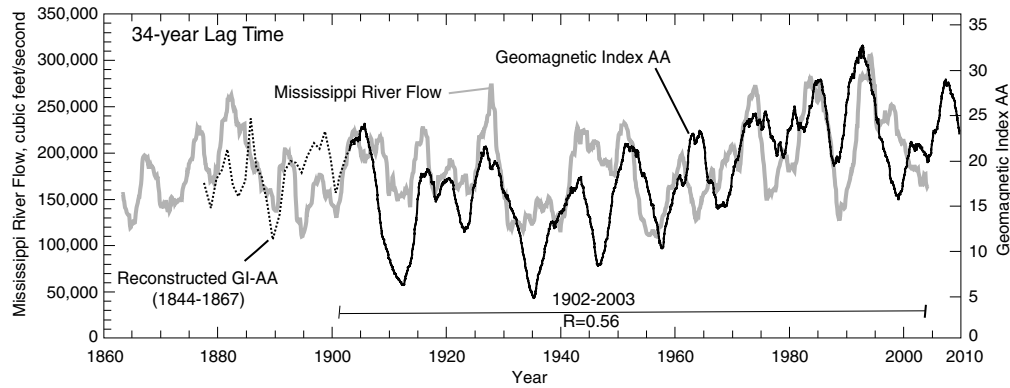


Fig. 7. Thirty-six month moving average of Mississippi River flow at St. Louis, Missouri, and geomagnetic index aa, lagged 34 years. Correlation for 1902–2003 based on June value of 36-month moving averages.

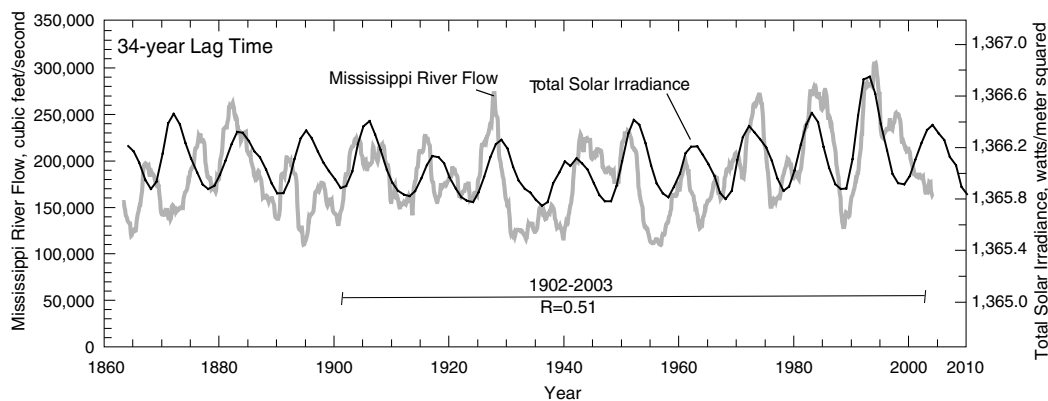


Fig. 8. Thirty-six month moving average of Mississippi River flow at St. Louis, Missouri, and total solar irradiance, lagged 34 years. Correlation for 1902–2003 based on June value of 36-month moving averages.

There are a few cases where peaks in the GI-AA were not a graphical match with peaks in the Mississippi River flow. Most notable is the wet period around 1882. The GI-AA shows the period bounded by two relatively weak peaks. Also, there could be a decrease in the lag time during the period 1950 to about 1980 by a few years.

The relation between Mississippi River flow and TSI for the period 1863 through 2003 is shown in Fig. 8. The lag time is 34 years, and the correlation between the data sets is $R = 0.51$ for the period 1902–2003. An interesting note is that where the GI-AA did not have a graphical match with the Mississippi River flow, for example around 1882, the TSI matches very well. Also, there is a tendency for the lag time to increase a year or two after 1970. This is consistent with the GI-AA data. Other highs and lows in TSI correspond to wet and dry years in the Mississippi River Basin. Neither the GI-AA nor the TSI gives a perfect match with streamflow, but they may be acting together in complex manner.

8. GI-AA and TSI combination

Care should be taken when trying to extrapolate variations of TSI and GI-AA data into future flows of the Mis-

issippi River. This paper suggests a connection between streamflow and TSI and GI-AA variations. The graphs and correlations show that the relations are not consistent and the lag time is not static. However, the visual correlation is remarkable, and a solar signature is definitely reflected in the Mississippi River flow.

The irradiance (TSI) and geomagnetic data (GI-AA) were scaled and combined according to the equation

$$\text{Combination} = 10 + 20,000 * ((\text{TSI} - 1365.918) / 1365.918) + (\text{GI-AA}). \quad (1)$$

This equation resulted in a value in which GI-AA approximately had twice the contribution to the combined value than the TSI. Comparisons of the combination data set and Mississippi River flow are shown in Fig. 9. The correlation with 1902–2003 Mississippi River flow ($R = 0.60$) was better than either of the individual components (Fig. 9A). When a 3-year slowing of the lag time is applied in 1977 (Fig. 9B), the correlation was even better ($R = 0.66$).

The apparent lag time between the solar signal and the climate response of the Mississippi River is over three decades. Also, the comparisons of solar data with the Mississippi River flow data show patterns that at times are a

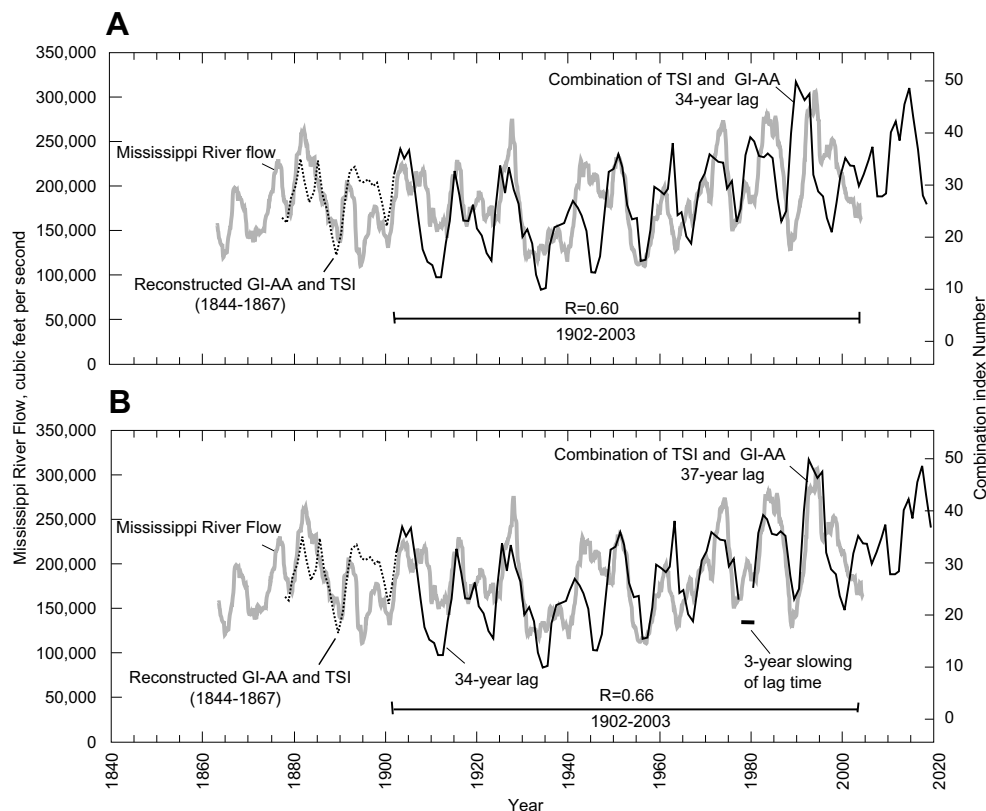


Fig. 9. Thirty-six month moving average of Mississippi River flow at St. Louis, Missouri and (A) combination of geomagnetic index aa and total solar irradiance, 34-year lag, and (B) combination (GI-AA/TSI) with 34- and 37-year lags. Correlations for 1902–2003 based on June value of 36-month moving averages.

couple of years ahead (circa 1962) or a couple of years behind (circa 2000) the 34-year lag. A possible cause of these time discrepancies could be changes in the velocity of the medium that is carrying the solar signal. That medium may well be the world's ocean conveyor belt system.

9. Ocean conveyor belt system

The ocean conveyor system is a vast interconnection of near-surface and deeper ocean currents that are thought to be driven by a thermohaline circulation (Broecker, 1991). Velocities within the conveyor are variable with highest velocities in the North Atlantic Ocean (Gulf Stream) and slowest in the Pacific Ocean. Vast amounts of water move through the conveyor, and its circulation traditionally is thought to take approximately a millennium for one round trip. The pump for the conveyor has been shown to be in the North Atlantic where warm salty ocean water gives up its heat to the atmosphere, sinks and flows south at depth and becomes the North Atlantic deep water (NADW). Approaching Antarctica, it turns east becoming the Circumpolar Current. Once in the Pacific Ocean, the circulation takes it across the Equator where it rises diffusely in the North Pacific (Broecker, 1991). Here, the ocean surface water interacts with the atmosphere to affect climate over North America.

Somewhere along this circulation, most likely flowing from the western tropical Pacific Ocean to the Indian Ocean in the area of the Indonesian flowthrough area (Fig. 1), the ocean could absorb varying amounts of energy from the sun. Variations in clouds, solar radiation, winds, and surface currents create ocean temperature and salinity anomalies that can be traced along various parts of the conveyor (Favorite and McLain, 1973; Ray and Wilson, 2003; Belkin, 2004). The total lifetime of these anomalies are unknown; however, there appears to be a memory of almost 3.5 decades between solar variations and North Pacific SSTs that can affect the Mississippi River flow. If the conveyor's velocity increases or decreases from various internal factors, the lag time between solar signal and Mississippi River flow also could vary. This changing lag time is evident in comparing TSI, GI-AA, and their combination data with Mississippi River flows. All three data sets show increasing lag times in the last two decades, which suggests a slowing of the ocean conveyor that supplies water that is diffusely rising in the North Pacific. There also is evidence that the ocean conveyor belt is also slowing in the Atlantic (Bryden et al., 2005).

Additionally, various properties of the ocean conveyor belt are still unknown (Wilson, 2001). The westward flow of warm water from the Indian Ocean around the Cape of Good Hope by the Agulhas Current is known to be

interrupted by the much colder, eastward flowing Benguela Current (Fig. 1). This interaction could have an effect of shunting some of the ocean temperature anomalies back eastward into the ocean current that ultimately rises in the North Pacific, thereby reducing the distance between energy input and subsequent energy release in the North Pacific. One property of the conveyor system is known; it is not a rigid or continuous system. If an adjustment for changing ocean conveyor belt velocity can be assumed, the fit between the GI-AA and TSI combination improves substantially (Fig. 9B).

10. Solar fingerprint in climatic time series

Solar activity and climatic time series correlations have been plagued by phase changes and relations that come and go. Nearly, all these types of analyses compare a solar variable directly with a climatic measurement on a direct cause-and-effect (0 lag time) basis. However, as seen with the GCR, GI-AA, and TSI analyses in this paper, the lag time with Mississippi River flow was shown to be approximately 34 years. If the ocean conveyor belt is carrying the solar signal, different locations on the globe should have different lag times.

Seven climatic time series from around the globe were compared with the solar time series to test this hypothesis. Fig. 10A–K presents these climatic time series that appear to have different lag times with the solar data (A, TSI/GI-AA combination; I, GCRs; J, GI-AA; and K, TSI). Because the solar signal and the climatic responses do not follow a pure sine wave but instead have similar amplitudes in the same change in time, a characteristic “fingerprint” can be seen when the data are stacked. Most notable is the 17-year period between solar peaks occurring in 1892 and 1909 and then only 8 years to the next peak (1917). Much like the location of the Fraunhofer absorption lines of hydrogen in stellar spectrographs can provide information on the speed at which a star is moving toward or away from the Earth (Huggins, 1868), these fingerprints may provide information on the lag time between when solar energy is added to the conveyor belt and when it is released to the atmosphere at various regions to produce rainfall and runoff.

An all India rainfall index (Fig. 10B; methodology developed by Sontakke et al., 1992) is a measure of monsoon strength where higher numbers correspond to greater monsoon rainfall. Data are available for 1813–1998. This time series shows a 0-year lag time with increased solar energy coinciding with higher monsoon rainfall. This feature also has been noted by Hiremath and Mandi (2004). Streamflow for the Vaal River in southeast Africa (Fig. 10C; Alexander, 2005) suggests a 17-year lag time. Bahia Blanca, Argentina, rainfall, (Fig. 10D; Global Historical Climatology Network, 2006) shows a 25-year lag time. Northeast Brazil rainfall (Fig. 10E; National Oceanic & Atmospheric Administration, 2006) also shows a 25-year lag time. Detrended North Pacific SSTs from 20° to 50° lat-

itude (Fig. 10F; Scripps Institute of Oceanography Library, 2002) show a 32-year lag time, whereas Mississippi River flow (Fig. 10G; US Geological Survey (2006)) shows a 34-year lag time. There is an interesting connection between the India rainfall index peaks in the early 1800s and the historic flood stages on the Mississippi River in 1844 and 1857, 1858, and 1862. There is also a data set from the Labrador Sea (Fig. 1) which is the principal component analysis of sea ice (Fig. 10H, Deser et al., 2002), whose fingerprint fits into a 70-year lag time. If this lag time is correct, the ocean conveyor belt may supply increasingly warmer water to the Arctic for the next several decades.

When these lag times are plotted on the ocean conveyor belt (Fig. 11), there seems to be a consistent progression of lag times if some of the warm current east of Africa is incorporated into the Circumpolar Current in the southern hemisphere (Fig. 11). Other climatic time series worldwide need to be examined in light of this varying lag-time feature. The result could be a better understanding of the climate system as well as the properties of the ocean conveyor system.

11. Summary and conclusions

A physical connection between total solar irradiance (TSI) and regional climate of central North America represented by Mississippi River flow at St. Louis, Missouri, has been demonstrated for the period 1950 through 2000. The connection displayed an apparent 3-year lag time between the solar signal and the streamflow response. However, the favorable correlation did not persist when streamflow data back to 1862 were included. The entire period of streamflow data had a much better correlation with the solar data when a lag time of 34 years was considered and galactic cosmic ray (GCR) and Geomagnetic index aa (GI-AA) data were included with the TSI. GI-AA is inversely related to GCR flux.

The physical processes associated with this connection between solar activity and streamflow are diagrammed in Fig. 12. The total amount of solar energy reaching the Earth's surface may be controlled through an interaction between TSI and GCRs, where high (low) GCR flux promotes cloudiness (clear skies) and higher (lower) albedo at the same time that TSI is lowest (highest) in the solar cycle. This combined effect then may have an effect on the amount of energy that could be absorbed by Earth, and specifically, its oceans. If this energy is absorbed at a strategic location within the ocean conveyor belt system, the temperature anomalies generated could be transported to locations where regional climate could be affected. The temperature of the North Pacific Ocean has shown a robust effect on upper-level pressure patterns above, which in turn affects low-level pressure patterns and the amount of precipitation in the Mississippi River basin. The current drought (1999–2006) in the Mississippi River basin appears

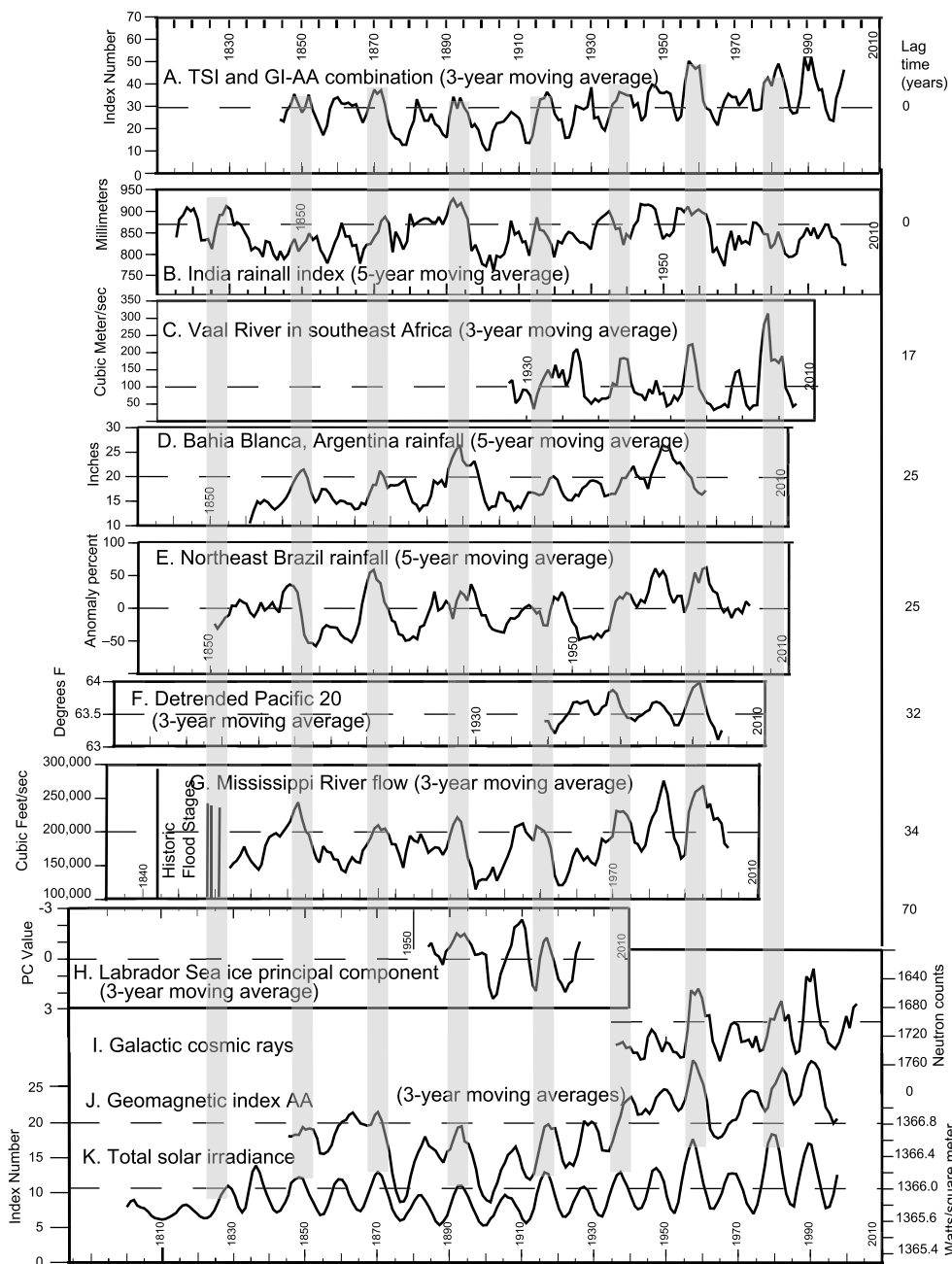


Fig. 10. Lag times between solar forcing from (A) combination of geomagnetic index aa and total solar irradiance, (I) galactic cosmic rays, (J) geomagnetic index aa, and (K) total solar irradiance, and climatic time series (B) all India Rainfall Index (Sontakke et al., 1992), (C) Vaal River flow in Southeast Africa (Alexander, 2005), (D) Bahia Blanca, Argentina, rainfall, (Global Historical Climatology Network (GHCN), 2006), (E), northeast Brazil rainfall (NOAA, 2006), (F) detrended North Pacific Sea-Surface Temperatures 20–50° latitude (Scripps Institute of Oceanography Library, 2002), (G) Mississippi River flow at St. Louis, Missouri, (US Geological Survey, 2006), and (H) Labrador Sea ice principle component analysis (Deser et al., 2002). Three- and 5-year moving averages applied as indicated on the graph.

to be caused by a period of lower solar activity that occurred between 1963 and 1977.

There appears to be a solar “fingerprint” that can be seen in climatic time series in other regions of the world, with each series having a unique lag time between the solar signal and the hydroclimatic response. The Indian Monsoon also follows the TSI/GI-AA interaction closely with greater rainfall over India coinciding with greater solar energy input into the Indonesian flowthrough area. A pro-

gression of increasing lag times can be spatially linked to the ocean conveyor belt, which transports the solar signal over a time span of several decades. This delay may be the reason that many solar/climate correlations break down when additional data become available. Because the solar cycles can vary from 8 to 12 years the normally selected 0-year lag time may be an incorrect choice. These solar/climate studies may be vindicated if longer lag times are incorporated.

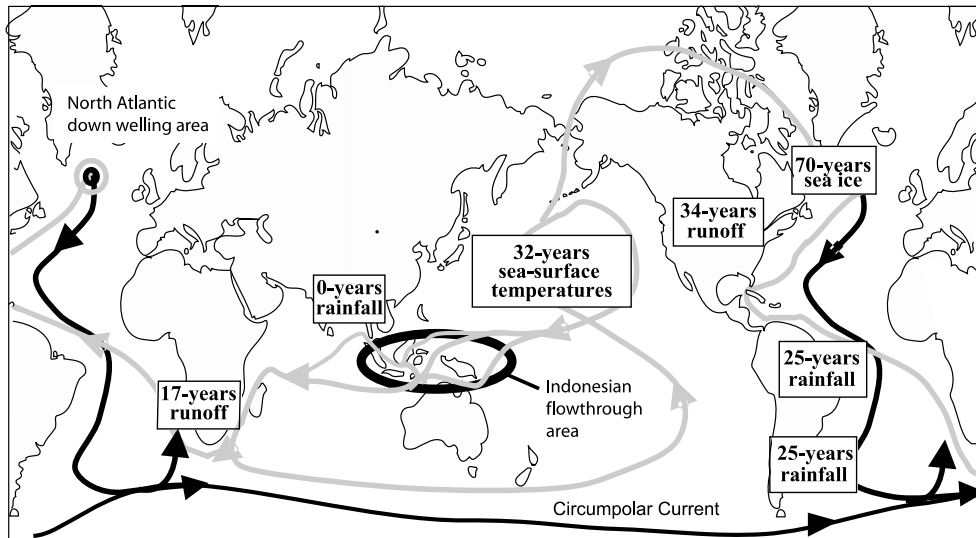


Fig. 11. Ocean conveyor belt and estimated lag times between solar signal and various regional climate time series.

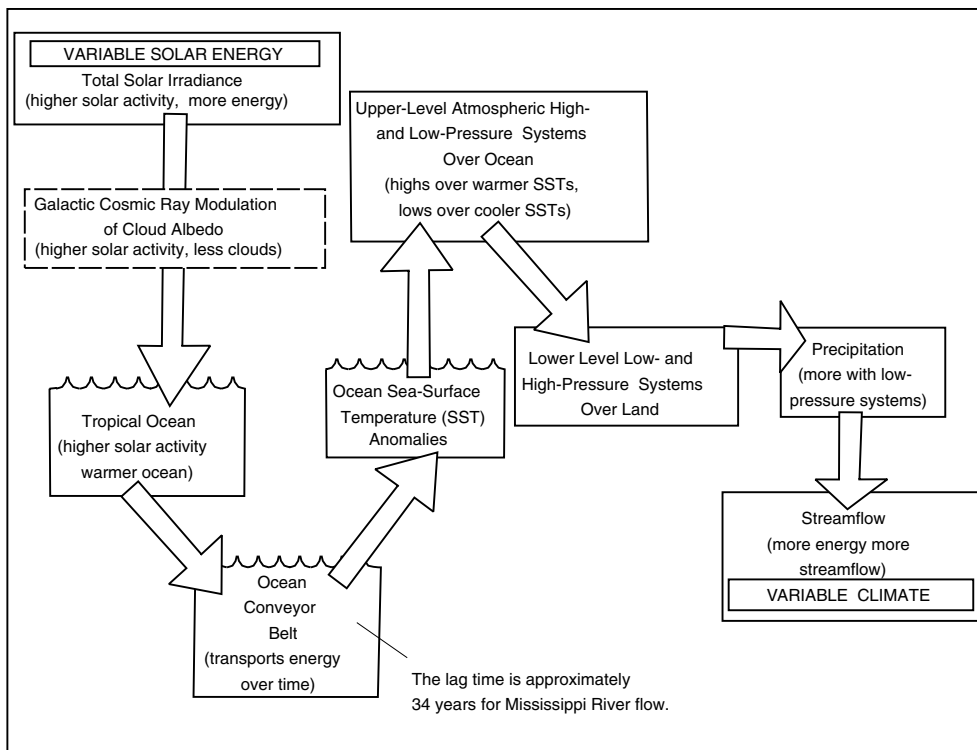


Fig. 12. Schematic diagram of energy flow from variable solar energy input to variable climate output.

There also may be a connection between slightly varying lag times for any one region and the strength or velocity of the ocean conveyor belt system. Velocities within the ocean conveyor belt are thought to be dependent upon temperature and salinity patterns in the world's oceans. In the North Atlantic Ocean the thermo-haline pump is known to modulate the relative velocity of the conveyor system in the North Atlantic with high (low)

salinity and cold (warm) sea-surface temperatures increasing (decreasing) conveyor velocities. If the velocities within the conveyor vary, the lag time between solar input and atmospheric response could vary. The TSI-GCR/streamflow relation shows an increasing time lag between solar data and Mississippi River flow at St. Louis, Missouri, since 1975, which suggests a slowing of the ocean conveyor system.

Temperature anomalies carried by the ocean conveyor belt system may be manifested in regional climatic time series worldwide. The lag time between the solar activity variations (input) and regional climate variations (output) appears to be a function of the travel time between the source of the ocean temperature anomalies (possibly the Indonesian flowthrough area) and the oceanic region that affects the atmospheric patterns that in turn control the climate for that particular region.

References

- Alania, M.V., Iskra, K., Modzelewska, R., Siluszyk, M. The galactic cosmic ray intensity and anisotropy variations for different ascending and descending epochs of solar activity, in: Proc. 29th International Cosmic Ray Conference, Pune, India, 2, pp. 219–222, 2005.
- Alexander, W.J.R. Development of a multiyear climate prediction model. *Water SA* 31 (2), 209–218, 2005.
- Belkin, I.M. Propagation of the “Great Salinity Anomaly” of the 1990s around the northern North Atlantic. *Geophys. Res. Lett.* 31, L08306, doi:10.1029/2003GL019334, 2004.
- Broecker, W.S. The great ocean conveyor. *Oceanography* 4, 79–89, 1991.
- Brooks, C.E.P. Variations in the levels of the Central African Lakes, Victoria and Albert. *Geophysical Memoirs*, 20, London (Meteorological Office), 1923.
- Bryden, H.L., Longworth, H.R., Cunningham, S.A. Slowing of the Atlantic meridional overturning circulation at 25 N. *Nature* 438, 655–657, 2005.
- Cliwer, E.W., Boriakoff, V., Feynman, J. Solar variability and climate change: geomagnetic AA index and global surface temperature. *Geophys. Res. Lett.* 25 (7), 1035–1038, 1998.
- Deser, C., Holland, M., Reverdin, G., Timlin, M. Decadal variation in Labrador Sea ice cover and North Atlantic sea surface temperatures. *J. Geophys. Res.* 107 (C5), 3035, doi:10.1029/2000JC000683, 2002.
- Favorite, F., McLain, D.R. Coherence in transpacific movements of positive and negative anomalies of sea surface temperature. *Nature* 244, 139–143, 1973.
- Foukal, P. Can slow variations of solar luminosity provide missing link between the Sun and climate: *Eos Trans. AGU* 84 (22), 205, 2003.
- Global Historical Climatology Network (GHCN). Precipitation data for Bahia Blanca, Argentina. <http://climvis.ncdc.noaa.gov/tmp/ghcn/13357.txt>, 2006.
- Hale, G.E. Sunspots as magnets and the periodic reversal of their polarity. *Nature* 113, 105, 1924.
- Hiremath, K.M., Mandi, P.J. Influence of the solar activity on the Indian monsoon rainfall. *New Astronomy* 9 (8), 651–662, 2004.
- Hoyt, D.V., Shatten, K.H. *The Role of the Sun in Climate Change*. Oxford University Press, Oxford, 1997.
- Huggins, W. Further observations on the spectra of some of the stars and nebulae, with an attempt to determine therefrom whether these bodies are moving towards or from the Earth, also observations on the spectra of the Sun and of Comet II. *Philos. Trans. R. Soc. Lond.* 158, 529–564, 1868.
- Kerthaler, S.C., Toumi, R., Haigh, J.D. Some doubts concerning a link between cosmic ray fluxes and global cloudiness. *Geophys. Res. Lett.* 26 (7), 863–865, 1999.
- Latif, M. Tropical Pacific/Atlantic Ocean interactions at multi-decadal time scales. *Geophys. Res. Lett.* 28 (3), 539–542, 2001.
- Latif, M., Barnett, T.P., Cane, M.A., Flugel, M., Graham, N.E., von Storch, H., Xu, J.-S., Zebiak, S.E. A review of ENSO predictions. *Climate Dyn.* 9 (4–5), 167–179, 1994.
- Lean, J. Evolution of the Sun’s spectral irradiance since the Maunder Minimum. *Geophys. Res. Lett.* 27 (16), 2425–2428, 2000.
- Lean, J., Beer, J., Bradley, R. Reconstruction of solar irradiance since 1610: implications for climate change. *Geophys. Res. Lett.* 22 (23), 3195–3198, 1995.
- Mass, C.F., Kuo, Y.H. Regional real-time numerical weather prediction: current status of future potential. *Bull. Am. Meteor. Soc.* 79 (2), 253–263, 1998.
- Mayaud, P.-N. The aa indices – a 100-year series characterizing the magnetic activity. *J. Geophys. Res.* 77, 6870–6874, 1972.
- McCabe, G.J., Dettinger, M.D. Decadal variations in the strength of ENSO teleconnections with precipitation in the western United States. *Int. J. Clim.* 19 (13), 1399–1410, 1999.
- McCabe, G.J., Palecki, M.A., Betancourt, J.L. Pacific and Atlantic Ocean influences on multidecadal drought frequency in the United States. *Proc. Natl. Acad. Sci.* 101, 4136–4141, 2004.
- National Geophysical Data Center. Galactic cosmic ray data, Huancayo, Peru. ftp://ftp.ngdc.noaa.gov/STP/SOLAR_DATA/COSMIC_RAYS/huancayo.tab, 2006a.
- National Geophysical Data Center. Geomagnetic index aa. ftp://ftp.ngdc.noaa.gov/STP/GEOMAGNETIC_DATA/AASTAR/aaindex, 2006b.
- National Geophysical Data Center. Sunspot number. ftp://ftp.ngdc.noaa.gov/STP/SOLAR_DATA/SUNSPOT_NUMBERS/, 2006c.
- National Oceanic & Atmospheric Administration, Earth System Research Laboratory. Northeast Brazil rainfall anomaly. <http://www.cdc.noaa.gov/Correlation/brazilrain.data>, 2006.
- Nevalinna, H. Results of the Helsinki magnetic observatory 1844–1912. *Ann. Geophys.* 22, 1691–1704, 2004.
- Palle, E., Butler, C.J. The influence of cosmic rays on terrestrial clouds and global warming. *Astro. Geophys.* 41 (4), 18–22, 2000.
- Palle, E., Butler, C.J., O’Brien, K. The possible connection between ionization in the atmosphere by cosmic rays and low level clouds. *J. Atmos. Solar Terrestrial Phys.* 66, 1779–1790, 2004.
- Perry, C.A. Midwestern streamflow, precipitation, and atmospheric vorticity influenced by Pacific sea-surface temperatures and total solar-irradiance variations. *Int. J. Clim.* 26 (2), 207–218, 2006.
- Ray, Patrick, Wilson, J.R. Long-term predictions of global climate using the ocean conveyor. *US DOE J. Undergraduate Res.* 3, 26–32, 2003.
- Roldugin, V.C., Tinsley, B.A. Atmospheric transparency changes associated with solar wind-induced atmospheric electricity variations. *J. Atmos. Solar Terrestrial Phys.* 66, 1143–1149, 2004.
- Rosenberg, R.L., Coleman Jr., P.J. Heliographic latitude dependence of the dominant polarity of the interplanetary magnetic field. *J. Geophys. Res.* 74 (24), 5611–5622, 1969.
- Scripps Institute of Oceanography. North Pacific Sea Surface Temperature Monthly Means, 1947 to 2001 (psstmv1.dat). Climate Research Division, 2002.
- Shindell, D., Rind, D., Balachandran, N., Lean, J., Lonergan, P. Solar cycle variability, ozone, and climate. *Science* 284, 305–308, 1999.
- Sontakke, N.A., Pant, G.B., Singh, N. Construction and analysis of All-India summer monsoon rainfall series for the longest instrumental period: 1813–1991. *Indian Inst. Trop. Meteorol. Research Report No. RR-053*, 1–22, 1992.
- Stuiver, M., Quay, P.D. Changes in the carbon-14 attributed to a variable Sun. *Science* 207, 11–19, 1980.
- Sun, B., Bradley, R.S. Solar influences on cosmic rays and cloud formation: a reassessment. *J. Geophys. Res.* 109, D14205, doi:10.1029/2001JD00560, 2002.
- Svensmark, H., Friis-Christensen, E. Variations of cosmic ray flux and global cloud coverage – a missing link in solar–climate relationships. *J. Atmos. Solar Terrestrial Phys.* 59, 1225–1232, 1997.
- Svensmark, H., Pedersen, J.O.P., Marsh, N.D., Enghoff, M.B., Uggerhoj, U.I. Experimental evidence for the role of ions in particle nucleation under atmospheric conditions. *Proc. R. Soc. A* 463, 385–396, 2007.
- US Geological Survey. Compilation of records of surface waters of the United States through September 1950, Part 7. Lower Mississippi River Basin. *US Geological Survey Water-Supply Paper* 1311, 23–24, 1956.
- US Geological Survey. National Water Information System. <http://waterdata.usgs.gov/usa/nwis/sw/>, 2006.
- Van Allen, J.A. *Cosmic Rays, the Sun and Geomagnetism: the works of Scott E. Forbush*. American Geophysical Union, Washington, 1993.

- Vine, F.J., Matthews, D.H. Magnetic anomalies over oceanic ridges. *Nature* 199, 947–949, 1963.
- Wang, Y.-M., Lean, J.L., Sheeley Jr., N.R. Modeling the Sun's magnetic field and irradiance since 1713. *Astrophys. J.* 625, 522–538, 2005.
- White, W.B., Cayan, D.R., Lean, J. Global upper ocean heat storage response to radiative forcing from changing solar irradiance and increasing greenhouse gas/aerosol concentrations. *J. Geophys. Res.* 103, 21355–21366, 1998.
- Willson, R.C. Total solar irradiance trend during solar cycles 21 and 22. *Science* 277, 1963–1965, 1997.
- Wilson, J.R. How fast is the conveyor? *World Resource Rev.* 13 (2), 199–220, 2001.